Article

Potential Exposure of Aquatic Organisms to Dynamic Visual Cues Originating from Aerial Wind Turbine Blades

Benjamin J. Williamson *[ID], Lonneke Goddijn-Murphy [ID], Jason McIlvenny [ID] and Alan Youngson

Environmental Research Institute, University of the Highlands and Islands, Ormlie Road, Thurso KW14 7EE, UK
* Correspondence: benjamin.williamson@uhi.ac.uk

Abstract: For many aquatic species, vision is important for detecting prey, predators, and conspecifics; however, the potential impacts of visual cues from offshore wind turbines have not been investigated in these crucial contexts. There is the possibility of visual cues, originating from moving wind turbine blades, propagating through the air–water interface to impact visually sensitive species. Two classes of visual cues are possible: direct motion cues originating as light reflected from moving turbine blades and indirect cues resulting from an interruption of direct sunlight causing dynamic shadowing when the sun, blade, and receptor are aligned. In both cases, the propagation of cues across the air–water interface is governed by physical principles but modulated in potentially complex ways by the aspects of the local environment that vary with time. Evidence for the extent of the exposure of aquatic organisms to the visual cues arising from moving turbine blades and for the potential response of receptor organisms is sparse. This study considers the physics involved to support the formulation and testing of robust biological hypotheses. Marine migratory salmonid species are considered as an example species because their behaviour in the marine environment is relatively well documented. This study concludes that the aquatic receptor organisms present in the uppermost layer of the sea in the vicinity of wind turbines are potentially exposed to direct motion cues originating from moving turbine blades and also, when the sun elevation angle is greater than ca. 20°, to dynamic shadowing cues.

Keywords: environmental impact assessment; wind turbine; direct motion visual cues; dynamic shadow cues; migratory salmonids

Key Contribution: Due to the increasing operation of wind turbines in marine environments, this study examines the physics underlying visual cues originating in reflected light from moving wind turbine blades propagating through the air–water interface. When the sun elevation angle is greater than ca. 20°, aquatic receptor organisms will also be exposed to dynamic shadowing cues. Consideration of physical principles will allow hypotheses to be formulated and tested to investigate any potential impacts on visually sensitive species present in the uppermost layer of the sea in the vicinity of wind turbines.

1. Introduction

The global drive towards offshore renewable energy requires an evaluation of the potential effects on aquatic organisms [1]. Since the need for renewable energy is considered to transcend many other considerations, Johnson et al. [2] have proposed using the construction and operational phases of renewable installations as de facto experiments that can be retrospectively evaluated to guide and improve future environmental policy on marine installations and engineering design.

Marine wind turbine arrays result in environmental alteration and ecological disturbance in the construction phase, the operation phase, and inevitably also the decommissioning phase. During the construction and decommissioning phases, the effects are likely to be highly dependent on local conditions and will have to be investigated in context.

However, the longer-lasting operational phase will be associated with generic effects on the marine environment that arise directly from the design and functionality of single turbines and turbine arrays. Possible systemic effects on the aquatic environment during operation include noise originating within the turbine nacelle, infrasound generated by the vibration of the turbine tower, electromagnetic fields (EMFs) generated by the cables carrying a current, changes to the hydrodynamics and mixing, the introduction of a hard substrate for colonisation, and the impacts of direct visual cues and the dynamic shadows generated by moving turbine blades [3,4]. The investigation of the systemic effects is susceptible to a general approach, including experimental hypothesis testing, potentially providing information that can be shared among locations and applications. In the context of field experimentation, there is a need to consider all the candidate effects from the outset to guide data collection and facilitate a later evaluation free of the confounding effects.

As context, turbine rotor diameters are increasing as larger units are installed; as of 2023, the largest is a 16 MW unit with a 260 m rotor diameter at a hub height of 152 m, installed in the Fujian offshore wind farm in the Taiwan Strait (New Atlas [5], accessed 1 September 2023). In Scottish Waters, consent conditions often specify a minimum spacing between turbines, for example, >1000 m for the 10 MW 164 m diameter turbines at Seagreen 1 [6]. Turbine rotational speeds for these large machines are typically <15 rotations per minute (rpm), e.g., a 13.9 rpm maximum is used in Seagreen.

This study considers the physics underlying the propagation of visual cues from turbines (Section 2) to facilitate further consideration of the possible effects of moving blades on marine receptor organisms (Section 3). The most general case relates to the perception of temporal patterns generated by ambient light (scattered light and direct sunlight) reflected from moving turbine blades and perceived against the general background of incoming scattered light and sunlight. A special case arises when the sun, turbine, and receptor organism are in direct alignment. Under these conditions, any incoming visual cues in the aquatic space are dominated in high contrast by dynamic shadowing—the pulsed interruption of direct sunlight caused by the moving turbine blades.

2. Optical Oceanography

2.1. Natural Daylight Above the Water Surface

For understanding the phenomena of the reflection, refraction, and penetration of daylight, two components need to be distinguished, sunlight and skylight (Figure 1). Sunlight is directed while skylight is more diffused. For a clear sky, the percentage of skylight is determined by the solar elevation angle (Figure 1) and increases with a lowering sun [7]. The presence of clouds considerably changes the fraction (one for a completely overcast sky) and distribution of skylight. The percentage of skylight is wavelength dependent; it is greater with shorter wavelengths towards the blue end of the visible spectrum [7]. Reflectance of the solar beam and skylight must be treated differently; this is true for a water surface as well as for any other light-reflecting surface. Optically smooth surfaces (mirror-like) reflect a light beam and optically rough surfaces scatter light in many directions. If the water surface is perfectly smooth, the surface reflectance for direct sunlight is equal to the Fresnel reflectance, meaning the angle of reflectance equals the angle of incidence in the opposite direction [8].

For high solar elevation angles, the reflectance is near zero, being at 2% for normal incidence and increasing with a lowering sun angle (Figure 2). For diffuse skylight, the surface reflectance ranges from 6.6% (smooth sea, uniform sky) to 4.3% (rough sea, overcast sky) [7].
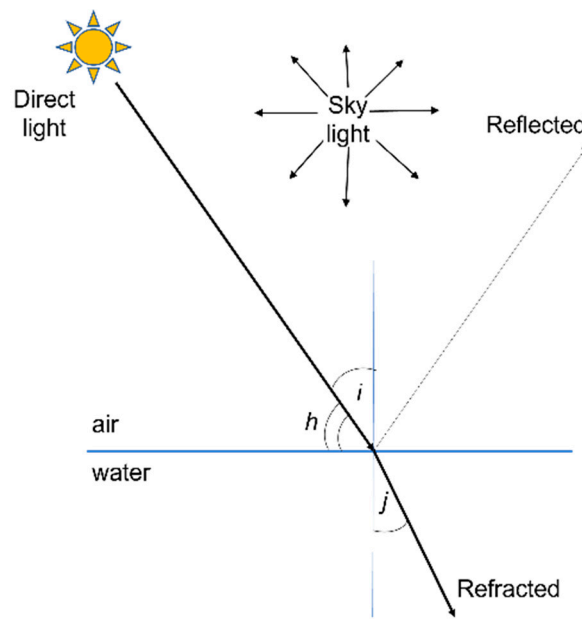
Figure 1. Diagram showing the composition of natural daylight and Fresnel reflection and the refraction of direct light (the solar beam) at a smooth water surface with solar elevation angle '*h*', angle of incidence '*i*', and angle of refraction '*j*' defined as being in the same plane.
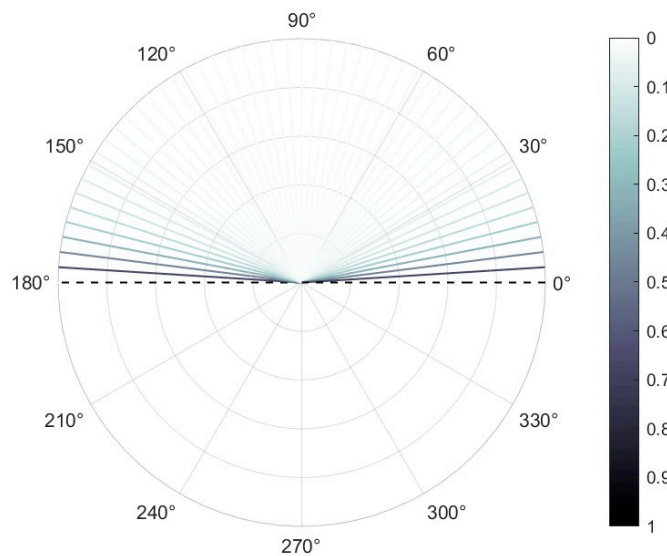

Figure 2. Diagram showing Fresnel reflectance. For $i = 0°$ to $70°$, Fresnel reflectance increases from 0.02 to 0.13 (and ultimately to 1 for grazing incidence, $i = 90°$, when all light is reflected).

2.2. Transmission of Light Across the Air–Water Interface

Light that is not reflected at the air–water interface is transmitted across it. Figure 1 illustrates how light entering a medium of a higher optical density (larger refractive index, *n*) is refracted towards the normal incidence so that the angle of refraction is smaller than the angle of incidence. For air $n = 1$ and for water $n = 1.33$, Snell's law determines that light of a grazing incidence ($i = 90°$) at a smooth water interface produces a critical angle of refraction, $j = 48.5°$ 9 [7,8]. As a result, all the light entering a water body is compressed into a cone of 97° (Figure 3), the so called 'Snell's window'. Because light at angles of incidence > 70° is mostly reflected (Figure 2), less is transmitted, dimming the edge of the Snell's window.
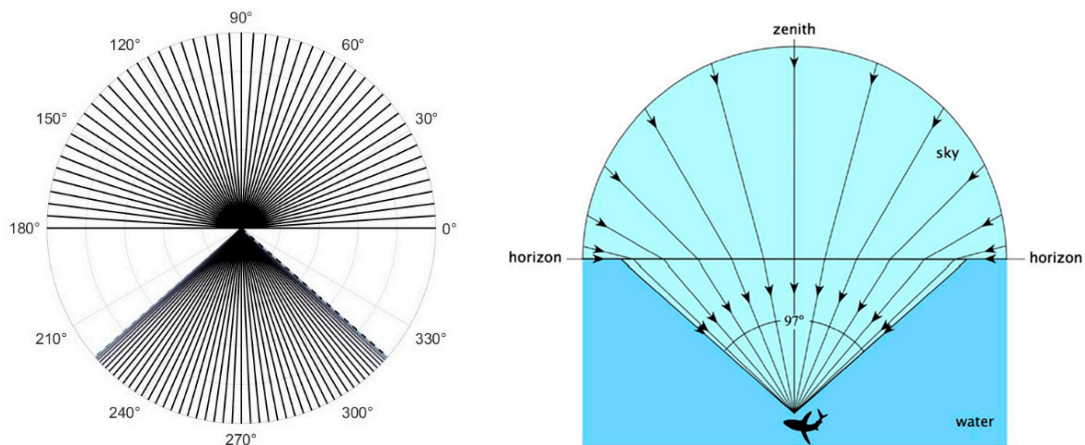
Figure 3. (**Left**)—diagram showing Fresnel refraction of light from the upper hemisphere into water; the dashed line indicates the critical angle (48.5°). (**Right**)—optics of Snell's window for flat water. Image taken from Lynch [9].

Another consequence of light refraction is that objects seen from beneath the water's surface look distorted and displaced (Figure 4).
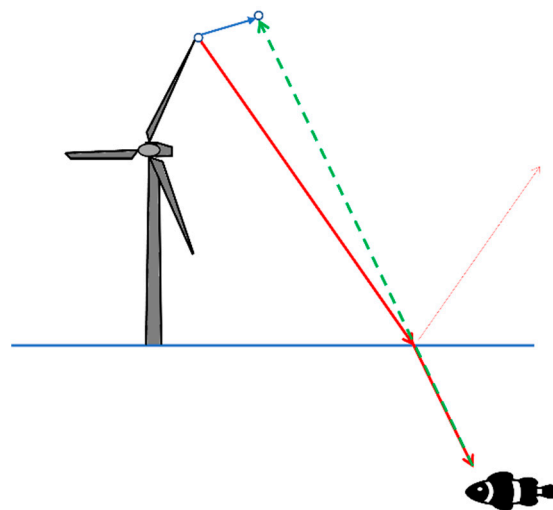

Figure 4. Diagram showing how light reflected from a point in the air (red line, here the tip of a wind turbine blade, with the wind turbine shown oblique to the page) transmitted across a smooth water surface appears closer to an aquatic receptor organism (green dashed line) due to refraction of light.

2.3. Underwater Light Climate

Light that enters an aquatic medium interacts with the water itself, dissolved organic matter, the photosynthetic biota, and inanimate particulate matter (tripton). Pure water absorbs very weakly in the blue/green parts of the spectrum (approximate wavelengths 450–570 nm) but absorbs quite significantly in the red part (620–750 nm), which explains the apparent blue colour of clear water on a sunny day [10]. Dissolved organic matter absorbs blue light (450–495 nm), making the water appear yellow and it is, therefore, sometimes called a 'yellow substance' or 'gilvin' (Kirk, 1983) [11]. Many solar photons are scattered one or more times by the water and its constituents before they are absorbed. This, and the removal of some of the photons that are scattered back upwards, contributes to vertical light attenuation. Subsurface upwelling light that crosses the water–air interface is confined to Snell's window (Figure 3) as all the light with a subsurface angle of incidence over 48.5° is reflected internally at the water–air interface.

The vertical attenuation coefficient K [m^{-1}] is a measure for the diminution of light, K_d for the downward irradiance. A related term is the optical depth (ζ), defined by the product of K_d and the depth (z). One optical depth (where $z = 1/K_d$) is the depth at which the downward irradiance falls to $1/e$ (37%) of the subsurface value. (Irradiance is the time rate flow of the radiant energy (radiant flux) received by a surface per unit area.) K_d may be approximated using the Secchi depth (Z_{sd}) by $1.44/Z_{sd}$, but this is sometimes very inaccurate (Kirk, 1983) [11]. Z_{sd} [m] is measured by lowering a white disc of 20–30 cm in diameter on a rope into the water and seeing at which depth it disappears from view. K_d is related to, but not the same as the beam attenuation coefficient c; in general, K_d is smaller than c [7].

2.4. Effect of Surface Roughening

A roughening of the water surface by surface wind changes the reflection and refraction of light, depending on the solar elevation angle. For high solar elevation angles, the angle of incidence will on average be increased. The effect of surface roughening for high solar elevation angles is negligible for reflectance, as reflectance varies little with the solar elevation if it is high (Figure 2). For low solar elevation angles (below 20°), however, reflectance is considerably reduced by surface roughening which explains why the sea looks darker with increasing winds [7], indicating that more light is transmitted across the air–water interface. For a rough surface, shadows and multiple reflections by waves become important factors when the sun is low [12]. Wave slopes greater than about one-half the angle of the sun elevation can cause a second reflection [13]. A natural slick or oil slick will reduce the wind roughening of a water surface [13].

Glitter is a special aspect of reflection that arises when a water surface is roughened by the wind, caused by wave facets reflecting sunlight to the receptor. Increasing roughness will enlarge the width of the glittering pattern. It is most pronounced at solar elevations of 30–35° and the pattern becomes narrower when the sun sets [7]. As seen from beneath the surface, the refracted glitter is confined to a smaller angle (Figure 3) and is of the order of 1000 times more intense than the reflected glitter [7]. Underwater visuals of a wind turbine against a cloudy sky (Figure 5) created using Blender, a free and open-source 3D computer graphics software toolset [14], illustrate Snell's window and the other optical phenomena discussed above. In addition, Figure 5 shows that increasing sea surface roughness degrades the spatial coherence of direct visual cues, and more especially, the spatial and temporal integrity of dynamic cues.
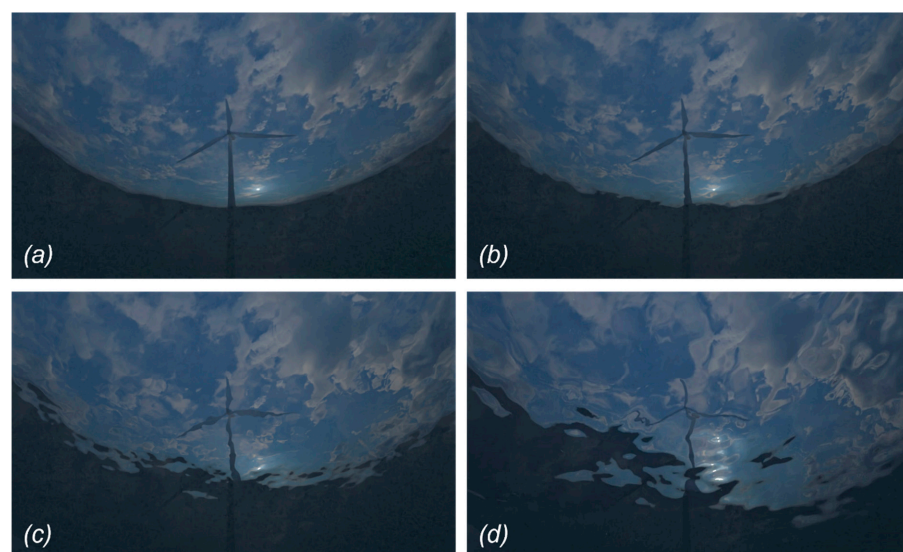

Figure 5. Visuals of a wind turbine from beneath the water's surface with increasing roughening of the water surface from a to d, created using Blender [14]. The figures show (**a**) no ripples, calm conditions, (**b**) 5 cm high ripples, (**c**) 10 cm high ripples, and (**d**) 25 cm high ripples. Viewpoint placed at 2 m water depth. The 60-m high wind turbine is approximately 250 m from the viewpoint position.

2.5. Geometry of Shadows

A rotating wind turbine can cast a moving shadow over a water surface causing underwater shadows and light flicker. The sweep area and contrast of the shadow depend on intensity of the sunlight, solar angles (elevation angle measured up from the horizon and azimuth angle measured clockwise from the north), the wind turbine's size, location and orientation (azimuth), water surface roughness, water depth, and water quality. The projection of a shadow onto a horizontal plane is fairly straightforward as the rays of the solar beam can be assumed to be parallel due to the far distance of the sun [8]. Solar angles can be retrieved from the NOAA Sunrise/Sunset and Solar Position Calculator (http://gml.noaa.gov/grad/solcalc/azel.html, accessed on 3 October 2024) and the Fresnel equations applied to the shadow rays to estimate transmission across the water surface (Figure 6). The lower the sun, the longer the shadows but also, the less transmission through the water surface in combination with a lower light intensity. The light flicker rate or shadow speed can be predicted from the rotation speed of the wind turbine.
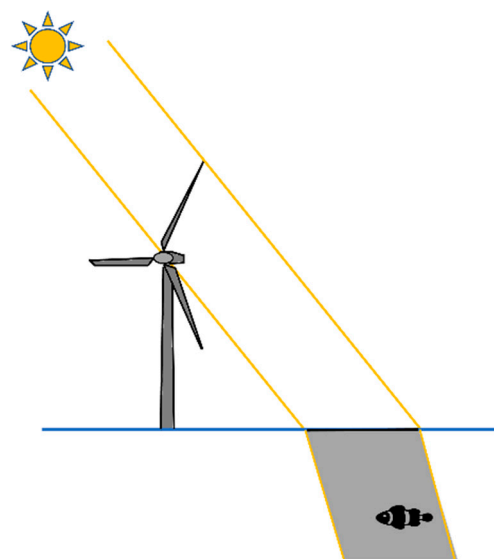

Figure 6. Shadow rays (in yellow) from a wind turbine blade traveling across a smooth water surface, with the wind turbine shown oblique to the page.

2.6. Visibility

The visuals of objects and their shadows depend on the perception of the differences in radiance (radiant flux received by a surface per unit solid angle and per unit area) leaving an object and its surroundings. Hence, the concepts of contrast and of contrast transmittance are important [7]. Contrast, *C*, often termed Weber contrast in the visual ecology literature [12], is defined by

$$C = \frac{L - L_b}{L_b}$$

with L [W m^{-2} sr] as the radiance emitted by an object and L_b as the uniformly radiant background [7]. For an ideal black object ($L = 0$) viewed against a radiant background, the contrast would be -1, varying to ∞ for a radiant object observed against an ideal black background ($L_b = 0$). In shallow epipelagic zones of the sea, a background radiance always exists due to the light scattering of the radiant object and of the prevailing daylight. Scattering through the path of sight to the eye results in a veil of light reducing the contrast [7]. If the field radiance falls below the threshold of the receptor organism, a contrast will not be perceived. How contrast is perceived also depends on the colour of the light, as different wavelengths evoke differing neural responses.

2.7. What an Underwater Receptor Organism Sees of the Hemisphere Above

An underwater receptor organism looking up sees the world above the water surface through a cone of 97° (Figure 3); this is Snell's window containing all angles smaller than the critical angle (Figure 3) [7]. For larger directions of view, the received light only consists of the subsurface upwelling light reflected back down at the water–air interface. As the internally reflected light levels are low compared to the downwelling light from above, this area is relatively dark. If the field of view of the receptor organism is larger than 97°, for example 180°, through the use of a fisheye lens, and if the receptor organism scans the sea surface above, the receptor organism sees the upper hemisphere through a round window surrounded by darkness (Figure 5). Because the underwater receptor organism's view of the scene above the surface is the primary concern of this study, the focus is on Snell's window and the dark area is not further discussed. The downwelling above-surface light with high angles of incidence is reflected more than it is transmitted (Figure 2), which causes the light intensity of its refraction to rapidly decrease as the refraction angle approaches 48.5° (Figure 3). Surface waves cause the edge of Snell's window to be ragged (Figure 5) and its angular diameter to widen. The maximum width varies from 97° for smooth water up to about 122° for nonbreaking waves, broadening to approximately 180° for breaking waves [9]. With a roughening of the sea surface, more skylight can be seen underwater, which may brighten the underwater view but does not map the hemisphere above [9].

As seen in Figure 4, the refraction of light towards the normal incidence 'pulls in' the view of the upper hemisphere and as the underwater receptor organism descends, the view of the hemisphere seen through Snell's window widens (while the size of the window looks the same for the receptor organism). Figure 7 illustrates what is captured of the upper hemisphere in Snell's window with the receptor organism at different depths.
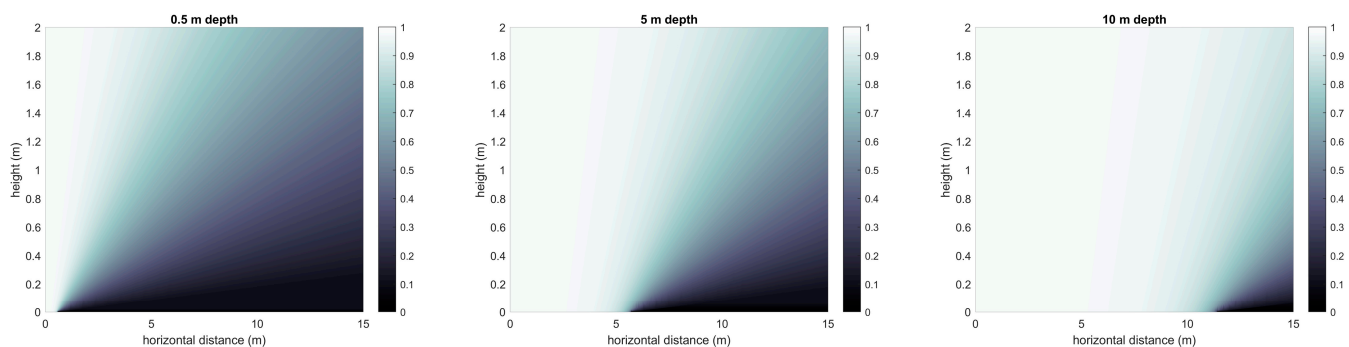

Figure 7. Transmission coefficient of light leaving a point at distance x and height z through an air–water interface for an underwater receptor organism at different depths (calculated using the Fresnel equations).

Once light is transmitted through the air–water interface, it is absorbed and scattered by water molecules and other organic and inorganic constituents, and more light is attenuated as it travels deeper. Figure 8 shows the light attenuation in Snell's window for different light attenuation coefficients (*c*) ranging from those that can be found, from left to right, in the open ocean, around the coast, and in the inland waters [11]. Wavelength dependence of the attenuation coefficient makes it different for different colours, i.e., some colours are attenuated more quickly than others depending on the water composition. As the underwater receptor organism descends, the edge of Snell's window and wave patterns near the edge soften while the brightness inside reduces [15]. For a complete understanding of what an underwater receptor organism sees, the Fresnel refraction (Figure 7) and subsurface light attenuation (Figure 8) need to be combined.
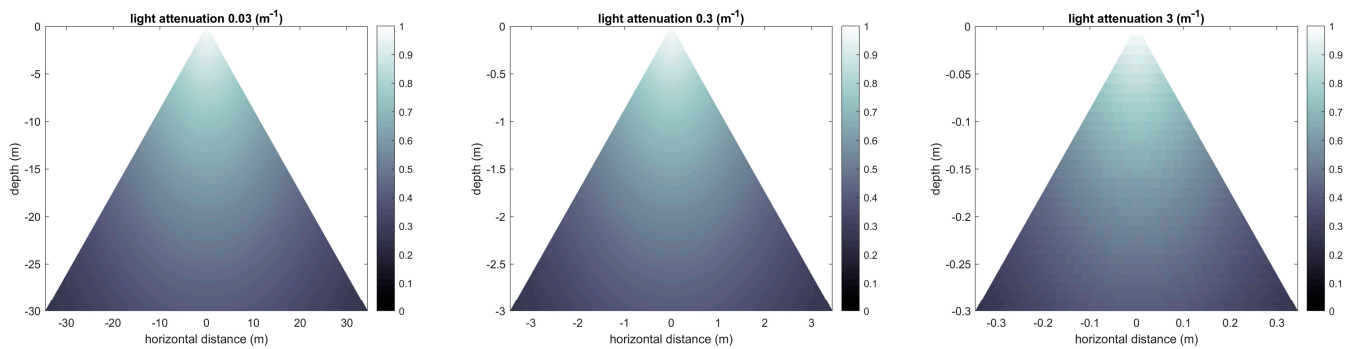
Figure 8. Attenuated light calculated as exp(-cL) with the light attenuation coefficient c (m^{-1}) and path length in water L (m).

3. Marine Migratory Salmonid Species

3.1. Receptor Organism Species

Marine migratory salmonid species are considered as a case study because their behaviour in marine environments is relatively well documented. Migratory salmonid species are widely distributed in the northern hemisphere. Many are regarded as an iconic species, and most are of substantial economic and social value. As a result, salmonids have been correspondingly well studied [16,17].

Many of the salmonid species undertake long return migrations between the rivers where they live as juveniles and their distant ocean feeding grounds. After a variable, species-dependent stay in freshwater, juvenile salmon leave their rivers for the ocean. Atlantic salmon (*Salmo salar*) smolts aged two or three years, for example, are commonly around 120–150 mm in body length making them suitable targets for study using small data tags. Those *Oncorhynchus* species that are fry migrants are much smaller and, therefore, harder to study. Adult salmonid fish of all species return to their rivers to spawn after a marine phase of, mostly, 1.5–2.5 years. Generally, adult migrants exceed 500 mm in body length at this stage and are, therefore, suited to behavioural studies based on emerging tag technologies.

3.2. Swimming Depths

The use of pressure-sensitive tags has made it possible to estimate the swimming depths of salmon during their marine migrations. Davidsen et al. [18] tracked hatchery-reared Atlantic salmon smolts in the deep fjordic waters of Norway; the mean swimming depth of individuals during daytime ranged from 0.5 to 2.3 m. Renkawitz et al. [19] reported that 95% of daytime detections of the hatchery-reared Atlantic salmon smolts migrating over deep water in Atlantic Canada were at a depth of <5 m. In eastern Scotland, Newton et al. [20] reported that the daytime mean value for the swimming depths of wild Atlantic salmon smolts migrating in the open sea was 1.0 m. No data appear to have been published for the swimming depth of smolts of the *Oncorhynchus* species in open coastal or ocean water.

For the case of adult fish, Holm et al. [21] reported that four Atlantic salmon individuals recaptured in Norway had previously been present at depths of <5 m for about 60% of the time as estimated for the oceanic phase of their marine migration. Godfrey et al. [22] reported the swimming depths for the return migration of wild Atlantic salmon in the northern coastal waters of Scotland. Thirty-four individuals spent 72% to 85% of the time at 0–5 m depths; during daylight hours, the values were biased towards shallower depths in this range. For the *Oncorhynchus* species, Ruggerone et al. [23] reported a mean swimming depth of 1.6 m for adult, steelhead trout (*Oncorhynchus mykiss*) in the coastal waters of British Columbia. Courtney et al. [24] tagged steelhead kelts leaving an Alaskan river and reported a mean swimming depth of 2.5 m during their subsequent time in the ocean. In an early study involving a small number of adult fish tagged in the Bering Sea, Ogura and

Ishida [25] showed the average daytime swimming depths for pink (*O. gorbuscha*), sockeye (*O. nerka*), and chum (*O. keta*) salmon of 10 m or less. The equivalent value for chinook salmon (*O. tshawytscha*) was greater at ca. 30 m, pointing to a possible species difference. In line with this, Smith et al. [26] compared the seasonal values for the mean swimming depths of the adult coho and chinook salmon in Puget Sound; for the coho salmon, the values were < ca. 10 m and they tended to be greater than the equivalent values for the chinook salmon. Candy and Quinn [27] reported mean daytime values of 25–64 m for the swimming depths of individual adult chinook salmon in the coastal waters. In particular, during both their outwards and inwards migratory phases, salmonids habitually transit through the surface layers of the ocean where they are potential receptor organisms of visual cues from rotating wind turbine blades.

3.3. Visual Cues

Visual cues generated in the air are transmitted into an aquatic environment through the air–water interface. The cues that pass through the interface are potentially available to aquatic receptor organisms possessing the capacity to perceive light. During daylight, marine receptor organisms are, therefore, potentially exposed to the novel, dynamic, visual cues generated by moving turbine blades. Radar tracking demonstrates that birds in flight near a marine windfarm find the visual stimuli generated by a turbine array, and by individual turbines, to be highly aversive [28]. Aquatic receptor organisms may respond in similar ways to subsurface cues, leading to an exclusion from marine space, including the blocking of movement or migration, especially for the epipelagic species habitually using the near-surface layers of the ocean.

Salmonids have a well-developed visual system that they use to detect both prey and potential predators. Nakano et al. [29] used physiological methods to characterise the visual system of masu salmon (*O. masou*), finding that the species has colour vision and is, therefore, sensitive to light over a wide range of wavelengths. The visual axis was found to be forwards and upwards, suggesting that Snell's window is prominent in the normal field of vision. The measured range of visual accommodation was large, stretching to infinity. However, fish are adapted to the visual confines of an aquatic environment in which the requirement for near-vision exceeds the need for far-vision. In line with this, fishes like salmonids facilitate distant focus by actively moving their eye lens from its resting position to be closer to the retina. In practice, because visual function in fish is biased in this way towards the detection of objects viewed at a relatively close range, distant objects viewed through Snell's window are unlikely to be perceived as sharp images. Consequently, any visual cues originating in distant aerial objects are more likely to be based on movement than on form. The visual acuity of masu salmon was reported to be high. Overall, therefore, Nakano et al.'s findings [29] suggest a capacity to perceive visual cues originating from above the surface and, in particular, to discern dynamic cues.

With regard to dynamic shadowing, the pulsed cues generated by strobe lighting are among the stimuli that have been tested in the applied context of fish guidance systems (reviewed by Noatch and Suski 2012; Jesus et al. [30,31]). The reported results are mixed, but for some species and wavelengths, the reaction of fish is aversive. It must be noted that the flicker frequencies deployed in strobe systems exceed the frequency of the flicker generated by turbines. A three-bladed turbine operating at a rotational speed of 15 revolutions per minute, for example, generates a blade-pass frequency, and a flicker frequency of only 0.75 Hz.

3.4. Fish Behaviour

Although the topic is under-researched, the presence of predators, or fear of predators, is considered to modify the behaviour of prey species through the so-called non-consumptive effects of predation [32]. If, for example, this is the case for aerial predation on fish species like salmonids, to which younger, smaller fish in near-surface waters are especially exposed [33], fish must assess the predation risk via the perception of visual cues that

somehow characterise potential predators. Likewise, dynamic subsurface shadowing may somehow suggest the proximity of aquatic predators. As suggested above, any generated cues are more likely to relate to the dynamic rather than the static aspects of the predator's presence and they are unlikely, therefore, to be predator-specific. It may, therefore, be asked whether the direct motion cues and/or dynamic shadow cues generated by moving turbine blades are also likely to signal risk, whether this perception directly alters the behaviour of species like salmonids, and to what extent any habituation may occur. The answers are presently unknown but discoverable and might be interpreted in the contemporary context developed by Palmer et al. [34].

In the related context of camouflage, Cuthill et al. [35] considered the effects of visual environmental noise, including caustics (dynamic light patterns caused by the refraction of light and subsequent convergence after passing through a rippled water surface) on prey detection by predators. They concluded that aquatic prey species should actively exploit noisy visual environments, where detection by predators is impaired, and that predators should hunt preferentially in low-noise environments.

Atwell et al. [36] used experimentation and the simulation of caustics to show that three-spined sticklebacks (*Gasterosteus aculeatus*) avoided visually noisy environments. Avoidance was not associated with increases in risk-averse behaviour. Instead, the authors concluded that the fishes' ability to identify potential prey and to forage efficiently was likely impaired by visual noise, causing them to spend less time in noisy locations. Since most prey species are themselves predators, this would suggest a range of competing options for individuals.

For our case study of salmon, any response to spatial variations in the visual noise caused by turbines blades may, therefore, extend beyond the direct detection of the presence of putative predators; it may also include the strategic behaviour directed towards concealment near the ocean surface where salmon have been shown to spend much of their time (Section 3.2) and where visual noise is inherently the greatest (even in the absence of turbines).

4. Discussion

Marine wind turbines add a novel, highly dynamic aspect to the otherwise slowly changing aerial environment around them. These changes are self-evident above the ocean surface but present also in the subsurface space because, as discussed in Section 2, light passes through the air–water interface generating direct motion or dynamic shadowing cues for potential aquatic receptor organisms. Different environmental conditions (notably lighting and sea state) and turbine properties have different consequences for direct motion and dynamic shadow cues (Table 1), which can be predicted using the laws of physics (Section 2).

Table 1. Factors controlling the visual impact on aquatic receptor organisms of rotating wind turbines and their relevance for direct motion and dynamic shadow cues as perceived by an underwater receptor organism.

Factor	Direct Motion Cue	Dynamic Shadowing Cue
Illumination	Controls turbine visibility against background	Depends on solar angles and fraction of direct sunlight
Proximity	Depth dependent	Depth dependent; reach varies with solar elevation
Turbine height	Higher is more visible at greater distance	Higher, shadow is located further from turbine
Sea surface roughness	Distorted image	Wider but weaker

The potential exposure of receptor organisms to these cues varies temporally. Dynamic shadow cues are generated only during periods of sunlight and substantial cues are only generated when the angle of solar elevation exceeds ca. 20° and the surface transmission

of light is correspondingly high (i.e., >85%). Dynamic shadow cues are, therefore, absent or weak for the transitional periods after dawn or before dusk. Additionally, around the winter solstice at latitudes above ca. 46°, the sun's daily maximum angle of elevation is less than 20°, limiting the possibility for substantial dynamic shadowing effects during this time. At 58° degrees latitude, for example, the affected period extends from late October to mid-February. With these qualifications, therefore, the presence of turbines, and resultant patterns of both the reflected light and shadow, results in a permanent modification of the local daytime environment over the decades-long duration of the operational phase of a windfarm.

Based on a consideration of the physical principles, it has been possible, in part, to predict where cues from moving aerial turbine blades will present to aquatic receptor organisms and to identify the ultimate constraints on the propagation of visual cues through Snell's window and downwards into the aquatic space. The physical environmental variables are important qualifiers. Most notably, the roughness of the sea surface increases reflectance at lower solar elevations, and absorption and the scattering limit of the downward passage of the incoming light. Receptor organism depth is, therefore, crucial in both these respects. The intensity of the cues will be greatest at lesser depths where there is the least absorption. Direct visual cues will also be more coherent at lesser depths where light scattering is the least and where Snell's window is relatively smaller and, therefore, inherently smoother. The cues resulting from dynamic shadowing are likely to be more spatially pervasive because the sea surface state and cue coherence (Figure 5) are not limiting factors. However, absorption and scattering will limit the propagation of dynamic shadow cues with increasing depth and the alternating light and shadow components will be viewed in greatest contrast nearest to the ocean surface.

Small differences in swimming depth are predicted to have a large effect on the strength of the external visual cues propagating downwards from the surface through the sea water. The depth sensor technology available for earlier studies of tagged fish lacked the high degree of accuracy desirable in the present context and determining swimming depth was not always the main focus of investigation. Even so, salmonid smolts and adult salmonids appear to make extensive use of the shallow surface layers of deep coastal or oceanic waters. At both life stages, therefore, it is likely that individuals exhibiting this bias are exposed to visual cues originating from turbines positioned on the routes that link their natal rivers with their marine feeding grounds.

If the reaction of receptor organisms to direct visual cues or flickers is aversive, then access to marine space may be reduced around turbines, delaying or disrupting passage for surface-dwelling migratory species such as salmon over those particular periods when the visual cues are discernible. Any disruption caused by single turbines is expected to be exacerbated within the arrays containing multiple turbines. Any disruption is expected to be cumulative if multiple arrays are encountered by long-distance migrants, although the extent of any habituation is unknown.

5. Conclusions

In conclusion, based on an evaluation of theory, it is suggested that wind turbines generate visual cues for aquatic receptor organisms and that the cues have the potential to be aversive. Further research is required to generate direct evidence, and here, we present the physics involved to support the formulation and testing of robust biological hypotheses to investigate the direct visual and flicker effects.

While this study has used migratory salmonids as a case study, further studies are required across species groups. If species, including other key prey species, are found to avoid wind turbines or to occupy deeper depths, then there is a potential for wider trophic effects, e.g., a greater energetic cost of foraging for seabirds and marine mammals diving deeper to reach prey species with lower prey availability. Or, conversely, reduced foraging in offshore wind farms by seabirds may mitigate some concerns regarding seabird collision risks. These complex interlinked issues require robust evidence, underpinned

by an understanding of the physical mechanisms described here, that will allow the transferability, scaling, and modelling of potential impacts to be determined.

References

1. Isaksson, N.; Scott, B.E.; Hunt, G.L.; Benninghaus, E.; Declerck, M.; Gormley, K.; Harris, C.; Sjöstrand, S.; Trifonova, N.I.; Waggitt, J.J.; et al. A paradigm for understanding whole ecosystem effects of offshore wind farms in shelf seas. *ICES J. Mar. Sci.* **2023**, fsad194. [CrossRef]
2. Johnson, A.F.; Dawson, C.L.; Conners, M.G.; Locke, C.C.; Maxwell, S.M. Offshore renewables need an experimental mindset. *Science* **2022**, *376*, 361. [CrossRef] [PubMed]
3. Lovich, J.E.; Ennen, J.R. Assessing the state of knowledge of utility-scale wind energy development and operation on non-volant terrestrial and marine wildlife. *Appl. Energy* **2013**, *103*, 52–60. [CrossRef]
4. Dodd, J.A.; Briers, R.A. The Impact of Shadow Flicker or Pulsating Shadow Effect, Caused by Wind Turbine Blades, on Atlantic Salmon (*Salmo salar*) CD2020_08. Scotland's Centre of Expertise for Waters (CREW). 2021. Available online: http://crew.ac.uk/publications (accessed on 3 October 2024).
5. New Atlas. Available online: http://newatlas.com/energy/worlds-largest-wind-turbine-myse-16-260/ (accessed on 1 September 2023).
6. Seagreen Development Specification and Layout Plan May 2020. Available online: http://marine.gov.scot/sites/default/files/owf_dslp.pdf (accessed on 1 September 2023).
7. Jerlov, N.G. *Optical Oceanography*; Elsevier Publishing Company: Amsterdam, The Netherlands, 1968.
8. Hecht, E.; Zajac, A. *Optics*; Addison Wesley Publishing Company, Inc.: Boston, MA, USA, 1973.
9. Johnsen, S. *The Optics of Life: A Biologist's Guide to Light in Nature*; Princeton University Press: Princeton, NJ, USA, 2012.
10. Kirk, J.T.O. *Light and Photosynthesis in Aquatic Ecosystems*; Cambridge University Press: Cambridge, UK; London, UK; New York, NY, USA, 1983; p. 401.
11. Cox, C.; Munk, W. Slopes of the Sea Surface Deduced from Photographs of Sun Glitter. UC San Diego: Scripps Institution of Oceanography. 1956. Available online: http://escholarship.org/uc/item/1p202179 (accessed on 3 October 2024).
12. Cox, C.; Munk, W. Measurements of the roughness of the sea surface from photographs of the sun's glitter. *J. Opt. Soc. Am.* **1954**, *44*, 838–850. [CrossRef]
13. Blender Online Community. Blender—A 3D Modelling and Rendering Package, Blender Foundation, Amsterdam. 2018. Available online: http://www.blender.org (accessed on 30 May 2023).
14. Lynch, D.K. Snell's window in wavy water. *Appl. Opt.* **2015**, *54*, B8–B11. [CrossRef]
15. Molkov, A.A.; Dolin, L.S. The Snell's Window Image for Remote Sensing of the Upper Sea Layer: Results of Practical Application. *J. Mar. Sci. Eng.* **2019**, *7*, 70. [CrossRef]
16. Aas, Ø.; Klemetsen, A.; Einum, S.; Skurdal, J. (Eds.) *Atlantic Salmon Ecology*; John Wiley & Sons: Hoboken, NJ, USA, 2010.
17. Quinn, T.P. *The Behavior and Ecology of Pacific Salmon and Trout*; University of British Columbia Press: Vancouver, BC, Canada, 2007.
18. Davidsen, J.G.; Plantalech Manel-la, N.; Økland, F.; Diserud, O.H.; Thorstad, E.B.; Finstad, B. Changes in swimming depths of Atlantic salmon Salmo salar post-smolts relative to light intensity. *J. Fish Biol.* **2008**, *73*, 1065–1074. [CrossRef]
19. Renkawitz, M.D.; Sheehan, T.F.; Goulette, G.S. Swimming depth, behavior, and survival of Atlantic salmon postsmolts in Penobscot Bay, Maine. *Trans. Am. Fish. Soc.* **2012**, *141*, 1219–1229. [CrossRef]

20. Newton, M.; Barry, J.; Lothian, A.; Main, R.; Honkanen, H.; Mckelvey, S.; Thompson, P.; Davies, I.; Brockie, N.; Stephen, A. Counterintuitive active directional swimming behaviour by Atlantic salmon during seaward migration in the coastal zone. *ICES J. Mar. Sci.* **2021**, *78*, 1730–1743. [CrossRef]

21. Holm, M.; Jacobsen, J.A.; Sturlaugsson, J.; Holst, J.C. *Behaviour of Atlantic Salmon (Salmo salar L.) Recorded by Data Storage Tags in the NE Atlantic—Implications for Interception by Pelagic Trawls*; ICES: Copenhagen, Denmark, 2006; ASC CM 2006/Q:12.

22. Godfrey, J.D.; Stewart, D.C.; Middlemas, S.J.; Armstrong, J.D. Depth use and migratory behaviour of homing Atlantic salmon (Salmo salar) in Scottish coastal waters. *ICES J. Mar. Sci.* **2015**, *72*, 568–575. [CrossRef]

23. Ruggerone, G.T.; Quinn, T.P.; McGregor, I.A.; Wilkinson, T.D. Horizontal and vertical movements of adult steelhead trout, Oncorhynchus mykiss, in the Dean and Fisher Channels, British Columbia. *Can. J. Fish. Aquat. Sci.* **1990**, *47*, 1963–1969. [CrossRef]

24. Courtney, M.B.; Miller, E.A.; Boustany, A.M.; Van Houtan, K.S.; Catterson, M.R.; Pawluk, J.; Nichols, J.; Seitz, A.C. Ocean migration and behavior of steelhead Oncorhynchus mykiss kelts from the Situk River, Alaska. *Environ. Biol. Fishes* **2022**, *105*, 1081–1097. [CrossRef]

25. Ogura, M.; Ishida, Y. Homing behavior and vertical movements of four species of Pacific salmon (*Oncorhyncus* spp.) in the central Bering Sea. *Can. J. Fish. Aquat. Sci.* **1995**, *52*, 532–540. [CrossRef]

26. Smith, J.M.; Fresh, K.L.; Kagley, A.M.; Quinn, T.P. Ultrasonic telemetry reveals seasonal variation in depth distribution and diel vertical migrations of sub-adult Chinook and coho salmon in Puget Sound. *Mar. Ecol. Prog. Ser.* **2015**, *532*, 227–242. [CrossRef]

27. Candy, J.R.; Quinn, T.P. Behaviour of adult chinook salmon (Oncorhynchus tshawytscha) in British Columbia coastal waters determined from ultrasonic telemetry. *Can. J. Zool.* **1999**, *77*, 1161–1169. [CrossRef]

28. Fox, A.D.; Petersen, I.K. Offshore wind farms and their effects on birds. *Dan. Ornitol. Foren. Tidsskr.* **2019**, *113*, 86–101.

29. Nakano, N.; Kawabe, R.; Yamashita, N.; Hiraishi, T.; Yamamoto, K.; Nashimoto, K. Color vision, spectral sensitivity, accommodation, and visual acuity in juvenile masu salmon Oncorhynchus masou masou. *Fish. Sci.* **2006**, *72*, 239–249. [CrossRef]

30. Noatch, M.R.; Suski, C.D. Non-Physical Barriers to Deter Fish Movements. *Environ. Rev.* **2012**, *20*, 71–82. [CrossRef]

31. Jesus, J.; Cortes, R.; Teixeira, A. Acoustic and light selective behavioral guidance systems for freshwater fish. *Water* **2021**, *13*, 745. [CrossRef]

32. Lima, S.L.; Dill, L.M. Behavioural decisions made under the risk of predation: A review and prospectus. *Can. J. Zool.* **1990**, *68*, 619–640. [CrossRef]

33. Hostetter, N.J.; Evans, A.F.; Payton, Q.; Roby, D.D.; Lyons, D.E.; Collis, K. A review of factors affecting the susceptibility of juvenile salmonids to avian predation. *N. Am. J. Fish. Manag.* **2023**, *43*, 244–256. [CrossRef]

34. Palmer, M.S.; Gaynor, K.M.; Abraham, J.O.; Pringle, R.M. The role of humans in dynamic landscapes of fear. *Trends Evol. Ecol.* **2022**, *38*, 217–218. [CrossRef] [PubMed]

35. Cuthill, I.C.; Matchette, S.R.; Scott-Samuel, N.E. Camouflage in a dynamic world. *Curr. Opin. Behav. Sci.* **2019**, *30*, 109–115. [CrossRef]

36. Attwell, J.R.; Ioannou, C.C.; Reid, C.R.; Herbert-Read, J.E. Fish avoid visually noisy environments where prey targeting is reduced. *Am. Nat.* **2021**, *198*, 421–432. [CrossRef]